

University of Groningen

## LL-37 and HMGB1 induce alveolar damage and reduce lung tissue regeneration via RAGE

Pouwels, Simon D.; Hesse, Laura; Wu, Xinhui; Allam, Venkata Sita Rama Raju; van Oldeniel, Daan; Bhiekhari, Linsey J.; Phipps, Simon; Oliver, Brian G.; Gosens, Reinoud; Sukkar, Maria B.

*Published in:*  
American Journal of Physiology - Lung Cellular and Molecular Physiology

*DOI:*  
[10.1152/ajplung.00138.2021](https://doi.org/10.1152/ajplung.00138.2021)

**IMPORTANT NOTE:** You are advised to consult the publisher's version (publisher's PDF) if you wish to cite from it. Please check the document version below.

*Document Version*  
Publisher's PDF, also known as Version of record

*Publication date:*  
2021

[Link to publication in University of Groningen/UMCG research database](#)

*Citation for published version (APA):*

Pouwels, S. D., Hesse, L., Wu, X., Allam, V. S. R. R., van Oldeniel, D., Bhiekhari, L. J., Phipps, S., Oliver, B. G., Gosens, R., Sukkar, M. B., & Heijink, I. H. (2021). LL-37 and HMGB1 induce alveolar damage and reduce lung tissue regeneration via RAGE. *American Journal of Physiology - Lung Cellular and Molecular Physiology*, 321(4), L641-L652. <https://doi.org/10.1152/ajplung.00138.2021>

### Copyright

Other than for strictly personal use, it is not permitted to download or to forward/distribute the text or part of it without the consent of the author(s) and/or copyright holder(s), unless the work is under an open content license (like Creative Commons).

The publication may also be distributed here under the terms of Article 25fa of the Dutch Copyright Act, indicated by the "Taverne" license. More information can be found on the University of Groningen website: <https://www.rug.nl/library/open-access/self-archiving-pure/taverne-amendment>.

### Take-down policy


If you believe that this document breaches copyright please contact us providing details, and we will remove access to the work immediately and investigate your claim.

Downloaded from the University of Groningen/UMCG research database (Pure): <http://www.rug.nl/research/portal>. For technical reasons the number of authors shown on this cover page is limited to 10 maximum.

RESEARCH ARTICLE

*Deconstructing Organs: Single-Cell Analyses, Decellularized Organs, Organoids, and Organ-on-a-Chip Models*

**LL-37 and HMGB1 induce alveolar damage and reduce lung tissue regeneration via RAGE**

 Simon D. Pouwels,<sup>1,2,3</sup> Laura Hesse,<sup>1,3</sup> Xinhui Wu,<sup>3,4</sup> Venkata Sita Rama Raju Allam,<sup>5</sup> Daan van Oldeniel,<sup>1</sup> Linsey J. Bhiexharie,<sup>1</sup> Simon Phipps,<sup>6</sup>  Brian G. Oliver,<sup>5</sup>  Reinoud Gosens,<sup>3,4</sup> Maria B. Sukkar,<sup>5</sup> and  Irene H. Heijink<sup>1,2,3</sup>

<sup>1</sup>Department of Pathology and Medical Biology, University of Groningen, University Medical Center Groningen, Groningen, The Netherlands; <sup>2</sup>Department of Pulmonology, University of Groningen, University Medical Center Groningen, Groningen, The Netherlands; <sup>3</sup>Groningen Research Institute for Asthma and COPD (GRIAC), University of Groningen, University Medical Center Groningen, Groningen, The Netherlands; <sup>4</sup>Department of Molecular Pharmacology, Faculty of Science and Engineering, University of Groningen, Groningen, The Netherlands; <sup>5</sup>Graduate School of Health, Faculty of Health, University of Technology Sydney, Ultimo, New South Wales, Australia; and <sup>6</sup>QIMR Berghofer Medical Research Institute, Herston, Queensland, Australia

**Abstract**

The receptor for advanced glycation end-products (RAGE) has been implicated in the pathophysiology of chronic obstructive pulmonary disease (COPD). However, it is still unknown whether RAGE directly contributes to alveolar epithelial damage and abnormal repair responses. We hypothesize that RAGE activation not only induces lung tissue damage but also hampers alveolar epithelial repair responses. The effects of the RAGE ligands LL-37 and HMGB1 were examined on airway inflammation and alveolar tissue damage in wild-type and RAGE-deficient mice and on lung damage and repair responses using murine precision cut lung slices (PCLS) and organoids. In addition, their effects were studied on the repair response of human alveolar epithelial A549 cells, using siRNA knockdown of RAGE and treatment with the RAGE inhibitor FPS-ZM1. We observed that intranasal installation of LL-37 and HMGB1 induces RAGE-dependent inflammation and severe alveolar tissue damage in mice within 6 h, with stronger effects in a mouse strain susceptible for emphysema compared with a nonsusceptible strain. In PCLS, RAGE inhibition reduced the recovery from elastase-induced alveolar tissue damage. In organoids, RAGE ligands reduced the organoid-forming efficiency and epithelial differentiation into pneumocyte-organoids. Finally, in A549 cells, we confirmed the role of RAGE in impaired repair responses upon exposure to LL-37. Together, our data indicate that activation of RAGE by its ligands LL-37 and HMGB1 induces acute lung tissue damage and that this impedes alveolar epithelial repair, illustrating the therapeutic potential of RAGE inhibitors for lung tissue repair in emphysema.

*COPD; emphysema; organoids; precision cut lung slices; RAGE*

**INTRODUCTION**

Chronic obstructive pulmonary disease (COPD) is a chronic and progressive lung disease, characterized by predominantly neutrophilic inflammation and abnormal lung tissue repair, leading to chronic bronchitis and/or emphysema with severe airflow limitation. COPD is caused by a combination of genetic factors and chronic exposure to noxious particles or gases, such as those from cigarette smoke, exhaust fumes, and environmental pollution. Currently available pharmacological therapies for COPD reduce disease symptoms, but do not halt or reverse alveolar tissue damage. To identify therapeutic targets that promote lung tissue regeneration, increased insight

into the molecular and cellular responses involved in lung tissue damage and the aberrant repair processes in COPD is urgently awaited.

The airway mucosal layer is the first to encounter inhaled insults causing mucosal epithelial cell damage. The release of damage-associated molecular patterns (DAMPs) from the damaged airway epithelium has been proposed as a key step in the development of airway inflammation and emphysema (1–4). DAMPs are host molecules released from damaged cells and cells undergoing necrotic cell death, that upon their release activate pattern recognition receptors (PRRs) expressed on various cell types to initiate innate and adaptive immune responses (5). The profile of DAMPs released upon cigarette smoke-

induced cellular damage may contribute to the susceptibility to develop chronic inflammation in COPD, as supported by our previous findings on the association between cigarette smoke-induced neutrophilic inflammation and DAMP release profile (6, 7). DAMPs that signal via the Receptor for advanced glycation end-products (RAGE), such as cathelicidin (LL-37) and high mobility group box-1 (HMGB1) are of particular interest, as higher levels of these DAMPs have been detected in serum, sputum, and bronchoalveolar lavage (BAL) of patients with COPD compared with healthy individuals (4, 8), and both were found increased during COPD exacerbations (2, 9).

RAGE ligation induces the activation of several downstream signaling pathways, including nuclear factor-kappa-light-chain-enhancer of activated B cells (NF- $\kappa$ B), activator protein 1 (AP-1), signal transducer and activator of transcription (STAT), and iron regulatory protein-1 (IRP-1) pathways, leading to a proinflammatory response (10–12). Moreover, RAGE has been shown to be involved in multiple facets of COPD pathophysiology (13–15). The gene encoding RAGE, *AGER*, has been identified as a susceptibility gene for COPD (16, 17). Furthermore, we have previously shown that genetic susceptibility determines the magnitude of inflammation upon RAGE activation, indicating that RAGE signaling may contribute to the susceptibility to develop inflammation and lung tissue damage in COPD (2, 7). Upon activation of RAGE, LL-37 and HMGB1 induce NF- $\kappa$ B-mediated proinflammatory responses (4), although their effects can also be mediated by Toll-like receptor 4 (TLR4) binding (18). Mice overexpressing RAGE spontaneously develop emphysema (19), whereas RAGE knockout mice and mice treated with a specific RAGE inhibitor were protected against both neutrophil elastase- and cigarette smoke-induced manifestations of emphysema, including airspace enlargement (20–23). However, it is unknown whether the effects on alveolar tissue damage are a secondary effect of RAGE-induced inflammation or directly caused by RAGE activation, leading to alveolar epithelial cell cellular damage and/or impaired repair. Upon damage, the alveolar epithelium is regenerated by proliferation of alveolar epithelial progenitors and their differentiation into alveolar type II (ATII) cells and subsequent differentiation into ATI cells that form the gas exchange units.

We hypothesized that RAGE ligands directly induce alveolar tissue damage and reduce alveolar epithelial repair responses and blockage of the RAGE pathway reduces alveolar tissue damage and enhances tissue repair responses. In addition, we hypothesized that the magnitude of RAGE-induced alveolar tissue damage is dependent on genetic susceptibility. To address this, we examined the effect of LL-37 and HMGB1 on airway inflammation and alveolar tissue damage in mice genetically susceptible or nonsusceptible for the development of emphysema. In addition, we investigated the role of RAGE in this response by using RAGE and TLR4 knockout mice. To assess the direct effect of LL-37 and HMGB1 on alveolar epithelial damage and repair responses, we used the ex vivo murine PCLS and organoid models as well as the human alveolar cell line A549.

## MATERIALS AND METHODS

### Mouse Models and Ethics

Experiments using A/J, NZW/LacJ and C57BL/6 mice were approved by the Institutional Animal Care and Use

Committee of the University of Groningen and experiments using the C57BL/6 wild-type, RAGE<sup>-/-</sup>, TLR4<sup>-/-</sup>, and RAGE<sup>-/-</sup>TLR4<sup>-/-</sup> knockout mice were approved by the University of Technology Sydney Animal Care and Ethics Committee (ETH19-3483). Knockouts were obtained as specified previously (24). A/J and NZW/LacJ mice were obtained as pathogen-free female 8-wk-old mice ( $n = 6$  per group; Jackson Laboratories, Bar Harbor, ME), whereas C57BL/6 mice ( $n = 8$ ) were purchased from the Animal Resource Center (Perth, Australia) and knockout mice were bred in the animal facility at the University of Technology Sydney on a C57BL/6 background. No data points were excluded as outliers. In agreement with a previously optimized protocol, all mice received a single treatment of LL-37 (67.4  $\mu$ g; #94261, Sigma-Aldrich, St Louis, MO), HMGB1 (30  $\mu$ g; disulfide HMGB1, HMGBiotech, Milan, Italy), or BSA (67.4  $\mu$ g; Sigma-Aldrich) in 50  $\mu$ L saline by intranasal administration under oxygen/isoflurane anesthesia (2). After 6 h, mice were euthanized and bronchoalveolar lavage (BAL) fluid and BAL cells were collected and stored at  $-80^{\circ}\text{C}$  until further use.

Lung tissue was formalin-fixed, paraffin-embedded, sectioned, and stained for hematoxylin and eosin before alveolar size was analyzed. Linear mean intersect (LMI) was measured by taking nine microscopic photographs of the parenchyma, free of airways and blood vessels, and analyzing them under a  $\times 20$  magnification. A grid with 21 vertical lines was placed on top of the microscopic photograph and the number of interceptions between the lines and the alveolar septum is counted as measure for the alveolar size. The LMI was calculated as  $(n \times l \times 2)/m$  in which  $n$  is the total number of lines, i.e., 21,  $m$  is the number of intersects, and  $l$  is the length of the individual lines as calculated with the scale of the microscopic photo.

Myeloperoxidase (MPO), keratinocytes-derived chemokine (KC), and neutrophil elastase (NE) were measured using ELISA, according to manufacturer's protocol (R&D Systems, Minneapolis, MN; Mouse Myeloperoxidase DuoSet ELISA, DY3667; Mouse Neutrophil Elastase/ELA2 DuoSet ELISA, DY4517; Mouse CXCL1/KC DuoSet ELISA, DY453). Double-stranded DNA (dsDNA) levels were measured using the Quant-iT PicoGreen dsDNA Assay Kit (Invitrogen, Waltham, MA).

### Organoids

Mouse lung organoids were prepared as described previously (25, 26). In short, CD31<sup>-</sup>/CD45<sup>-</sup>/EpCAM<sup>+</sup> epithelial cells were isolated from young adult murine lung tissue (C57BL/6; age 8–12 wk) excluding trachea using the QuadroMACS Separator (Miltenyi Biotec, Leiden, The Netherlands). Then, 10,000 CD31<sup>-</sup>/CD45<sup>-</sup>/EpCAM<sup>+</sup> cells were seeded together with 10,000 mouse lung fibroblasts in 100  $\mu$ L growth factor-reduced 1:1 diluted Matrigel (Corning Life Sciences BV, The Netherlands) for 7 days. Organoids were grown in Falcon inserts (Corning) in a 24-well plate containing 400  $\mu$ L of organoid media (DMEM/F-12 with 5% FCS, 1% penicillin/streptomycin, 1% glutamine, 1% amphotericin B, 0.025% epidermal growth factor (EGF), 1% insulin-transferrin-selenium, 0.01% cholera toxin, and 1.75 % bovine pituitary extract), medium was replaced every 2–3 days. Organoid cultures were stimulated

with 10  $\mu\text{g}/\text{mL}$  LL-37, 200  $\text{ng}/\text{mL}$  HMGB1 on *days 1, 3, and 5* after a medium change. Organoids were counted and size was measured on *day 7*. Afterward, organoids were fixed in acetone:methanol 1:1 and prepared for immunofluorescence staining. Characterization of the organoids was assessed by measuring prosurfactant protein C (SPC+) as marker for alveolar organoids and acetylated- $\alpha$  tubulin (ACT+) as marker for airway organoids.

### Precision Cut Lung Slices

C57BL/6 mice were euthanized under anesthesia of 1.5% isoflurane/ $\text{O}_2$  inhalation. Upon opening of the abdominal cavity, a small incision was made in the trachea on the anterior side of the thickest band of cartilage, in which a cannula was placed, secured with a tight knot. Lungs were carefully inflated, minimizing injection pressure, with UltraPure Low Melting Point Agarose solution (1.5%,  $\pm 1.5$  mL, Invitrogen, Waltham, MA). After inflation, lungs were placed on ice for 15 min to ensure agarose solidification and subsequently separated into individual lobes. Using a tissue slicer (Leica VT 1000 S Vibrating blade microtome, Leica Biosystems B.V., Amsterdam, The Netherlands), precision cut lung slices (PCLS) were prepared in 4% agarose gel columns, at a thickness of 450  $\mu\text{m}$ . PCLS were washed (4 times) and cultured in DMEM (Lonza, Basel, Switzerland) supplemented with 1 mM sodium pyruvate, 1% MEM nonessential amino acids, 1.5  $\mu\text{g}/\text{mL}$  amphotericin B, 45  $\mu\text{g}/\text{mL}$  gentamycin, and 1% penicillin/streptomycin in 12-wells culture plates. Each well contained 2–3 lung slices. Agarose-free PCLS were treated with 1  $\mu\text{g}/\text{mL}$  FPS-ZM1 (Sigma Aldrich, St. Louis, MO) for 1 h before stimulation with or without 20  $\mu\text{g}/\text{mL}$  LL-37 or 200  $\text{ng}/\text{mL}$  HMGB1 for 24 h and subsequently treated with/without 2.5  $\mu\text{g}/\text{mL}$  porcine pancreas elastase (Sigma Aldrich, St. Louis, MO) for 24 h. Afterwards the LMI was measured in hematoxylin/eosin-stained sections of the PCLS (27, 28).

### Electrical Resistance Measurements

Alveolar epithelial adenocarcinoma cells (A549), which were previously shown to express RAGE (29–31), were cultured over a period of 48–72 h (37°C at 5%  $\text{CO}_2$ ) in RPMI/10% FCS and seeded into arrays of the electric cell-substrate impedance sensing system (ECIS; Applied BioPhysics Inc., Troy, MI). RAGE was silenced using a commercially available RAGE specific esiRNA kit (Sigma-Aldrich, St. Louis, MO), containing a variety of RAGE siRNAs. Transfection was performed, according to a previously optimized protocol (7, 32), in the ECIS arrays using lipofectamine RNAiMAX transfection reagent (Invitrogen, Carlsbad) in Optimem (Gibco, Waltham, MA) medium. The universal negative control siRNA (Sigma-Aldrich, St. Louis, MO) was used as scrambled control. Transfection was performed 24 h after seeding and 48 h before wounding. Resistance was monitored in real time at a frequency of 400 Hz. One hour after stimulation with LL-37 (20  $\mu\text{g}/\text{mL}$ ) and/or preincubation (1 h) with FPS-ZM1 (1  $\mu\text{g}/\text{mL}$ ) cells were wounded by electroporation (30 s, using voltage pulses of 5 V and a frequency of 40 kHz). After wounding, cells were monitored for 20 h to assess the epithelial repair response.

### Statistics

Statistical significance between groups was determined using a Mann–Whitney  $U$  test. Statistical differences between conditions in the ECIS experiments were determined using a two-way ANOVA. A  $P$  value lower than 0.05 was considered statistically significant.

## RESULTS

### RAGE Ligand-Induced Airway Inflammation Is Dependent on Genetic Susceptibility

Previously, we showed that a single intranasal LL-37 exposure was able to induce neutrophilic airway inflammation in BALB/cByJ mice (2). Here, we selected a susceptible (A/J) and nonsusceptible (NZW/LacJ) mouse strain for the development of emphysema (33), to dissect whether HMGB1 or LL-37 induced inflammation and/or tissue damage contributes to the susceptibility to develop emphysema.

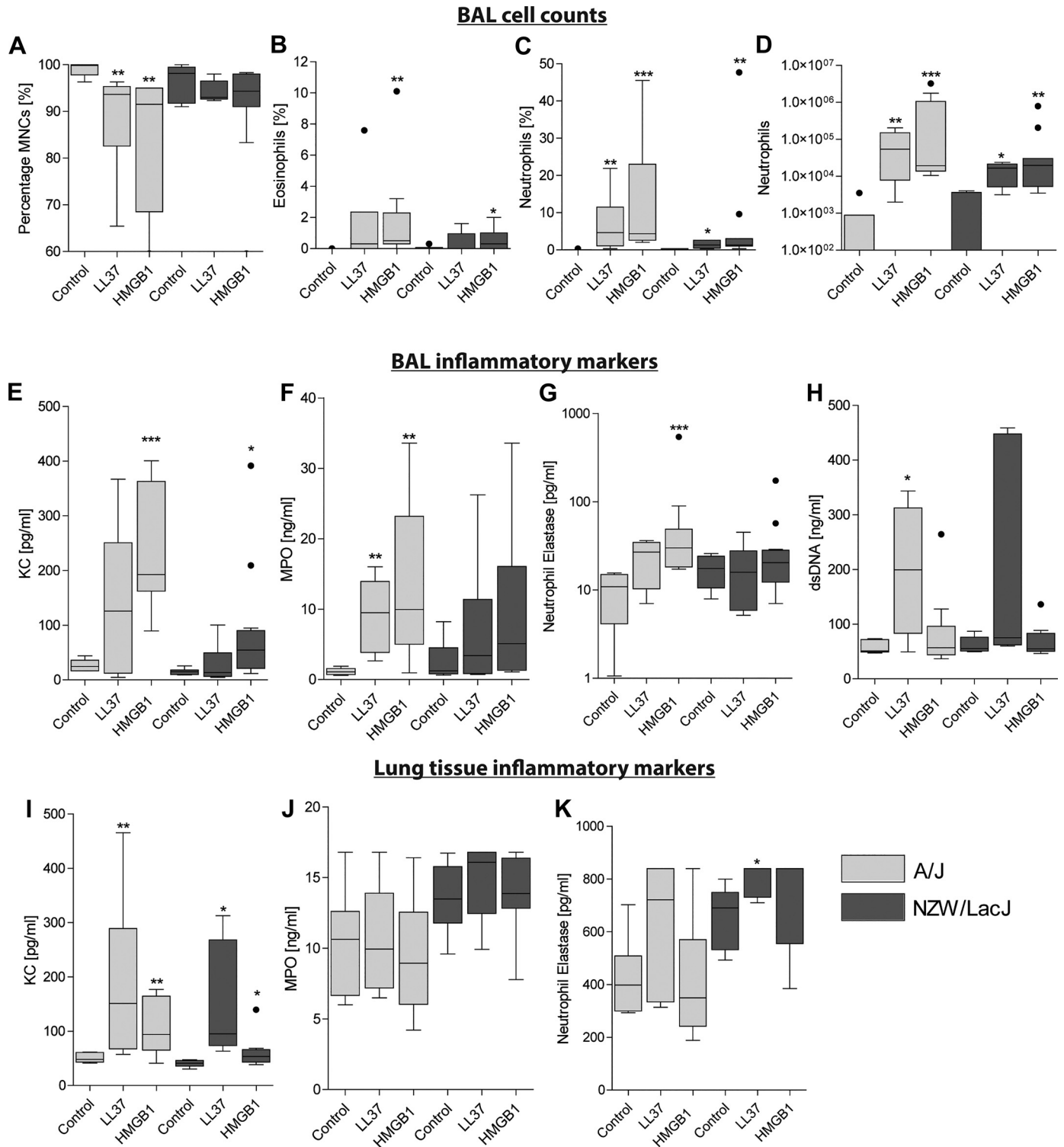
After 6 h, both HMGB1 and LL-37 induced a significant increase in neutrophil numbers in BAL fluid in both mouse strains (Fig. 1, C and D). In addition, HMGB1 but not LL-37, induced a significant increase in BAL eosinophil numbers (Fig. 1B) in both strains. Both HMGB1 and LL-37 induce a significant decrease in mononuclear cells in BAL fluid of A/J mice but not NZW/LacJ mice.

The BAL levels of the neutrophil chemoattractant KC were significantly increased upon HMGB1 treatment in both strains, whereas LL-37 treatment had no effect on BAL KC levels in either strain (Fig. 1E). The BAL levels of the neutrophilic inflammatory marker MPO were significantly increased by HMGB1 and LL-37 in A/J mice only (Fig. 1F). BAL levels of neutrophil elastase were increased upon treatment with HMGB1 but not LL-37 in A/J mice, whereas neither HMGB1 nor LL-37 had an effect on NE levels in NZW/LacJ mice (Fig. 1G). Increased BAL levels of the DAMP dsDNA, which serves as a marker of immunogenic cell death, were detected upon treatment with LL-37 in A/J mice only (Fig. 1H). No differences were found between LL-37- or HMGB1-treated and control mice for the DAMPs galectin-3 and HSP70 (data not shown).

In lung tissue homogenates, the levels of KC were increased upon treatment with both LL-37 and HMGB1 in both mouse strains (Fig. 1I). Lung tissue levels of MPO were not significantly increased upon treatment with HMGB1 nor LL-37 (Fig. 1, H–J). The lung tissue levels of NE were increased upon treatment with LL-37 in lung tissue of NZW/LacJ mice only (Fig. 1K).

When comparing the response to RAGE ligands in the susceptible A/J and the nonsusceptible NZW/LacJ strains, it is noteworthy that upon HMGB1 treatment the percentage of neutrophils in BAL fluid as well as the BAL levels of KC, MPO, and neutrophil elastase were significantly greater in A/J mice (Fig. 2). However, lung tissue levels of these mediators were comparable in A/J and NZW/LacJ mice. (Fig. 2, G–I).

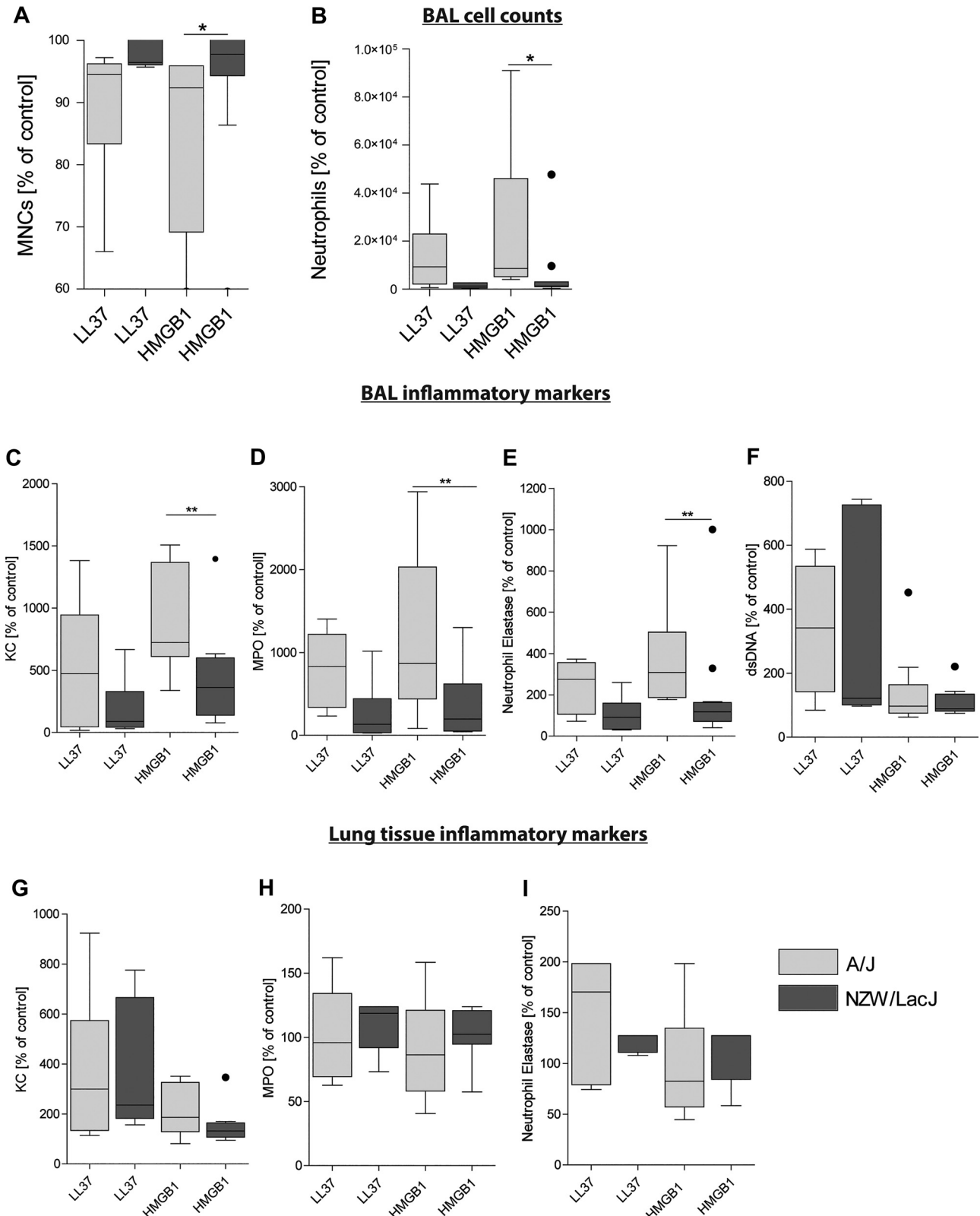
To determine whether the HMGB1- and LL-37-induced airway inflammatory responses are RAGE dependent, we assessed the effect of RAGE and TLR4 deficiency in C57BL/6 mice, which have been shown to be susceptible to the development of emphysema (33). We treated RAGE<sup>-/-</sup>, TLR4<sup>-/-</sup>,



**Figure 1.** The receptor for advanced glycation end-products (RAGE) ligands LL-37 and HMGB1, both induce airway inflammation upon intranasal treatment in mice. Mice genetically susceptible (A/J) or nonsusceptible (NZW/LacJ) for the development of emphysema were intranasally treated with a single-dose of the RAGE ligands LL-37 (67.4  $\mu$ g) and HMGB1 (30  $\mu$ g) or BSA (67.4  $\mu$ g) as control ( $n = 6-8$  per group). After 6 h, all mice were euthanized and broncho-alveolar lavage (BAL) fluid and lung tissue homogenate were analyzed for lung inflammatory markers. Inflammatory cells in BAL fluid were analyzed using the cytopsin cell differentiation assay. Mono-nuclear cells (percentage of total cells; **A**), eosinophils (percentage of total cells; **B**), neutrophils (percentage of total cells; **C**), and the absolute number of neutrophils (**D**) in BAL fluid is shown. Furthermore, the concentrations of the murine CXCL-8 analogue KC (**E**), myeloperoxidase (MPO; **F**), neutrophil elastase (NE; **G**) and dsDNA (**H**) were measured in BAL fluid. In lung tissue, homogenate the levels of KC (**I**), MPO (**J**), and NE (**K**) were measured. Data are expressed as box and Tukey whiskers ( $n = 6$  mice per group). Statistical differences were tested between the treatment groups and its corresponding control using the Mann-Whitney  $U$  test, where  $*P < 0.05$ ,  $**P < 0.01$ , and  $***P < 0.001$ . KC, chemokine.

and RAGE<sup>-/-</sup>TLR4<sup>-/-</sup> mice intranasally with HMGB1, LL-37, or BSA for 6 h. LL-37 induced airway inflammation in wild-type mice with a robust and significant increase in both macrophages and neutrophils whereas HMGB1 administration

did not lead to airway inflammation (Fig. 3). The LL-37-induced airway inflammatory response was completely absent in RAGE<sup>-/-</sup> mice whereas still present in TLR4<sup>-/-</sup> mice. The RAGE<sup>-/-</sup>TLR4<sup>-/-</sup> mice showed an intermediate



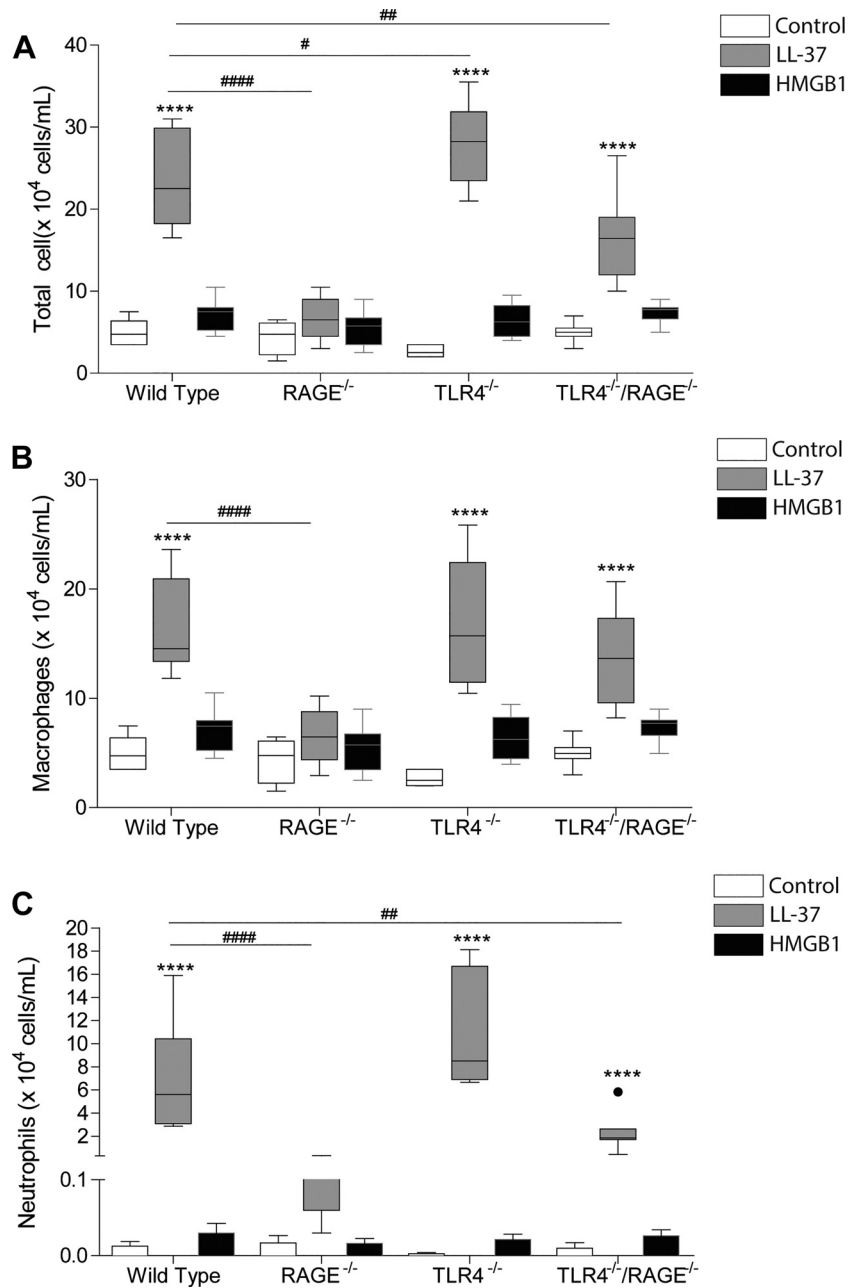


**Figure 3.** LL-37 induces acute airway inflammation upon intranasal injection in a receptor for advanced glycation end-products (RAGE)-dependent manner. Wild-type C57BL/6 mice and RAGE<sup>-/-</sup>, TLR4<sup>-/-</sup>, and TLR4<sup>-/-</sup>RAGE<sup>-/-</sup> mice on a C57BL/6 background ( $n=6-8$  per group) received a single intranasal treatment with LL-37 (67.4  $\mu$ g), HMGB1 (30  $\mu$ g), or BSA (67.4  $\mu$ g) as control. Six hours after the injection, mice were euthanized and BAL fluid was collected. The absolute number of white blood cells (A), macrophages (B), and neutrophils (C) was measured in BAL fluid. Data are expressed as box and Tukey whiskers,  $n=6-8$  mice per group. Significance was tested using a Mann-Whitney  $U$  test, \*\*\*\* $P < 0.0001$  between a treatment and the corresponding control treatment, # $P < 0.05$ , ## $P < 0.01$ , #### $P < 0.0001$  between mouse strains.

phenotype (Fig. 3). These data demonstrate that LL-37-induced airway inflammation is mediated by RAGE signaling.

### RAGE Ligands Acutely Induces Alveolar Tissue Damage in Mice

To investigate whether HMGB1 or LL-37 can induce alveolar tissue damage, airspace enlargement (LMI) was assessed

in mice after a single treatment with HMGB1 or LL-37. HMGB1, but not LL-37, induced a significant increase in airspace enlargement 6 h after treatment, in both the susceptible (A/J) as well as the nonsusceptible (NZW/LacJ) mouse strain (Fig. 4, A–B). In A/J mice, HMGB1 treatment induced a significantly larger increase in LMI compared with NZW/LacJ (Fig. 4C). Of note, the mean alveolar size at baseline

**Figure 2.** Mice susceptible for the development of emphysema develop stronger airway neutrophilic inflammation upon intranasal treatment with receptor for advanced glycation end-products (RAGE) ligands than nonsusceptible mice. Mice genetically susceptible (A/J) or nonsusceptible (NZW/LacJ) for the development of emphysema were intranasally treated with a single-dose of the RAGE ligands LL-37 (67.4  $\mu$ g) and HMGB1 (30  $\mu$ g) or BSA (67.4  $\mu$ g) as control ( $n=6-8$  per group). After 6 h, all mice were euthanized and broncho-alveolar lavage (BAL) fluid and lung tissue homogenate were analyzed for lung inflammatory markers. The relative difference between control mice and the RAGE ligand-treated mice are shown as percentage of mono-nuclear cells (A) and neutrophils (B) of control mice. The percentage increase of the murine CXCL-8 analogue KC (C), myeloperoxidase (MPO; D), neutrophil elastase (NE; E), and dsDNA (F) in BAL fluid compared with the mean of the control groups is shown. In lung tissue homogenate the percentage increase of KC (G), MPO (H), and NE (I) compared with the control groups is shown. Data are expressed as box and Tukey whiskers ( $n=6-8$  mice per group). Statistical differences were tested using the Mann-Whitney  $U$  test, where \* $P < 0.05$  and \*\* $P < 0.01$ . KC, chemokine.

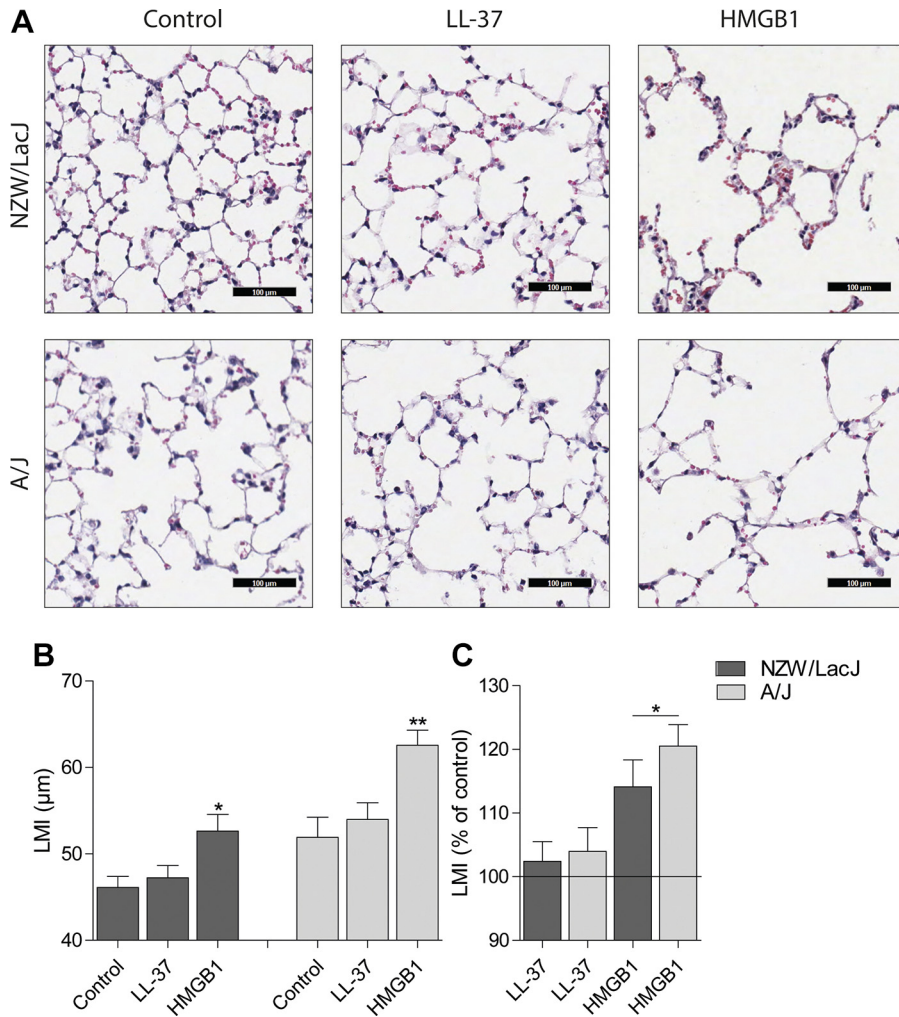


**Figure 4.** HMGB1 induces acute alveolar tissue damage in mice upon intranasal treatment in mice susceptible and nonsusceptible for the development of emphysema. **A:** hematoxylin and eosin staining on lung tissue of mice susceptible (A/J) or nonsusceptible (NZW/LacJ) for the development of emphysema, which received a single intranasal treatment with LL-37 (67.4 µg), HMGB1 (30 µg), or BSA (67.4 µg) as control ( $n=6$ /group). Black scale bars represent 100 µm. **B:** linear mean intersect (LMI) analysis as marker for lung tissue damage. **C:** the relative LMI is shown as percentage of the mean of the strain specific control group. Data are expressed as means  $\pm$  SE,  $n=6-8$  mice per group. Significance is tested using a Mann-Whitney  $U$  test, where  $*P < 0.05$  and  $**P < 0.01$ .

was larger in A/J mice, which may contribute to the higher susceptibility for the development of emphysema.

**RAGE Inhibition Prevents Elastase-Induced Alveolar Tissue Damage in Precision Cut Lung Slices**

To assess whether RAGE ligands directly induce alveolar damage, we used C57BL/6 murine PCLS, an ex vivo model that lacks any recruitment of circulating immune cells (Fig. 5A). PCLS showed substantial RAGE expression within the alveolar epithelium (Fig. 5B). Upon visual inspection, no obvious differences in RAGE expression were observed between untreated PCLS or PCLS treated with either LL-37 or HMGB1 (Fig. 5B). Stimulation of PCLS with LL-37 or HMGB1 led to significant alveolar enlargement (Fig. 5C). When the PCLS were preincubated with the RAGE inhibitor FPS-ZM1 before stimulation with LL-37 or HMGB1, the airspace enlargement was prevented, indicating that LL-37 and HMGB1 induce alveolar tissue damage via RAGE signaling. To model neutrophil elastase-induced emphysema, PCLS were ex vivo treated with porcine pancreas elastase for 24 h, which led to severe alveolar damage as indicated by a marked increase in alveolar size (Fig. 5D). Next, PCLS were treated with FPS-ZM1 either before or after the induction of tissue damage with elastase. Treatment of

PCLS with FPS-ZM1 after, but not before, the induction of lung tissue damage significantly reduced the airspace enlargement, suggesting that RAGE activation impairs lung tissue repair and/or regeneration upon elastase-induced damage.

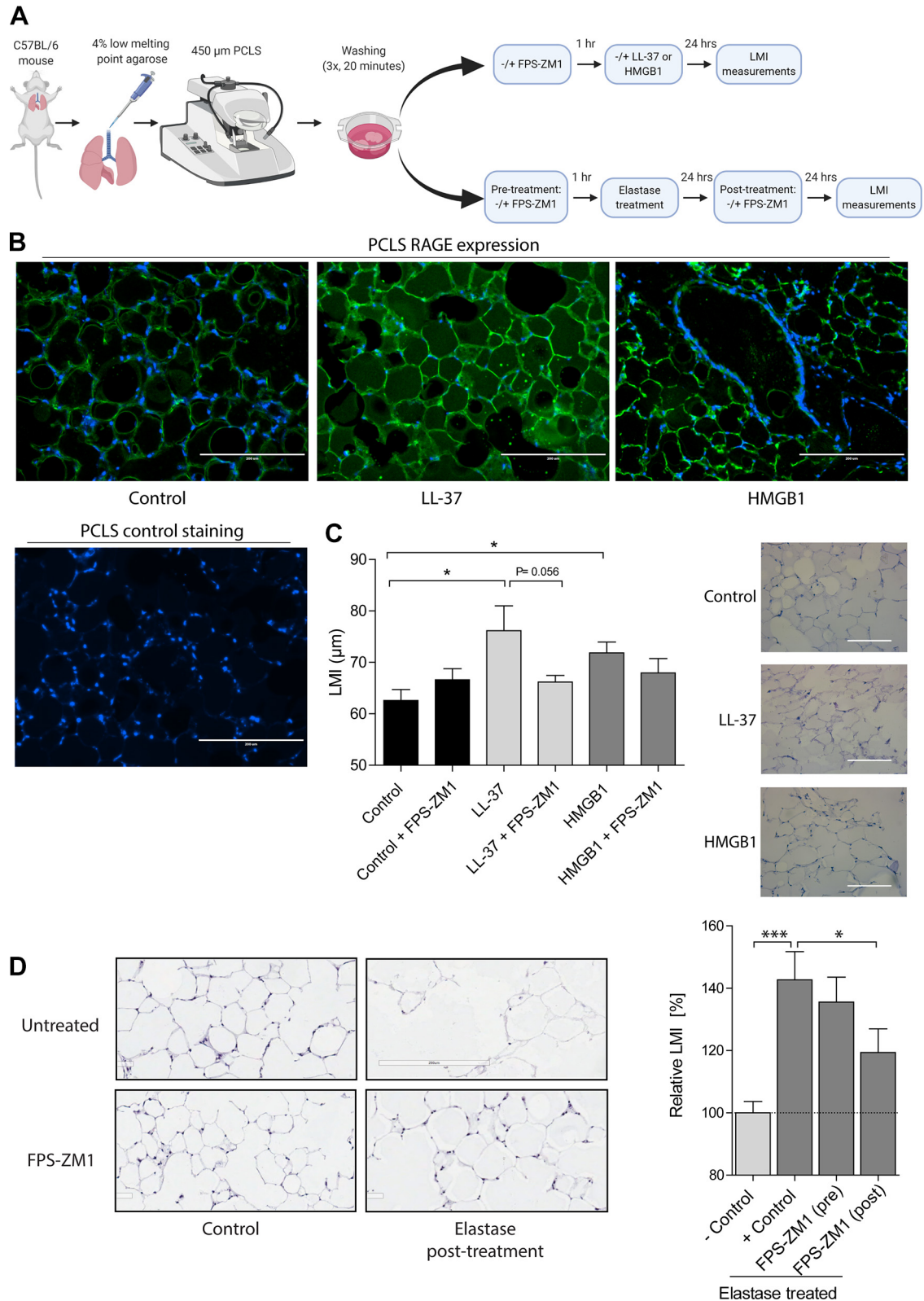
**RAGE Activation Affects Mouse Lung Organoid Growth and Organization**

To assess whether RAGE activation affects alveolar epithelial regenerative responses, we used an organoid model. Epithelial EpCAM<sup>+</sup> progenitors were seeded into Matrigel in the presence of fibroblast feeder cells to induce the formation of self-organized organoids. During the formation of organoids, LL-37 and HMGB1 were added to the culture every 48 h. Per well, between 30 and 35 organoids formed, with a morphology of grape-shaped alveolar or larger, more spherical airway structures (Fig. 6A; 25). Notably, after 7 days of culture in the presence of LL-37 or HMGB1, the total number of organoids was significantly reduced whereas the mean size of the organoids was considerably larger compared with the nonstimulated organoids (Fig. 6A). To assess the type of organoids formed upon LL-37 or HMGB1 stimulation, the organoids were stained for the ATII marker SPC and airway ciliated cell marker ACT. This analysis confirmed that the larger organoids



observed in LL-37 and HMGB1 stimulated cultures were indeed largely positive for ACT whereas the smaller organoids were negative for ACT and strongly SPC positive (Fig. 6B). Quantification of organoid size and number confirmed that

upon treatment with either HMGB1 or LL-37, there were significantly fewer organoids whereas the mean diameter of the organoids was increased (Fig. 6, C and D). These data suggest that RAGE ligands favor the growth of airway-derived



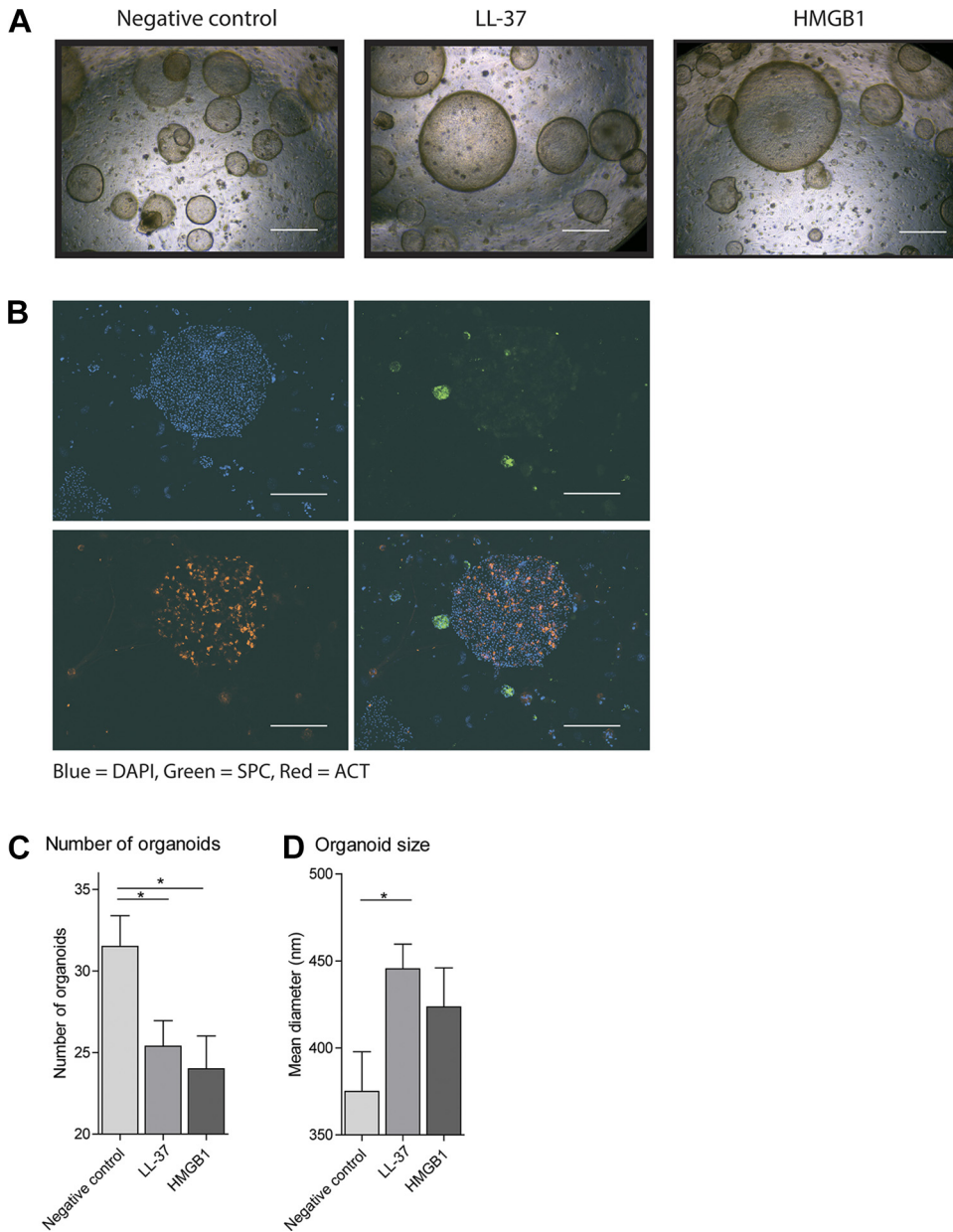


**Figure 6.** Mouse lung organoids are affected in size and number upon stimulation with receptor for advanced glycation end-products (RAGE) ligands. Mouse lung organoids were prepared by seeding 10,000 EpCAM<sup>+</sup> cells together with 10,000 MLg2908 mouse lung fibroblasts in 100  $\mu$ L growth factor-reduced 1:1 diluted Matrigel for 7 days. *A*: organoid cultures were stimulated with 10  $\mu$ g/mL LL-37 or 200 ng/mL HMGB1 on days 1, 3, and 5 after a medium change. Photos depict light microscopic images of organoids grown in Matrigel on a 24-wells insert. *B*: visual representation of the prosurfactant protein C<sup>+</sup> (SPC<sup>+</sup>) organoids as marker for alveolar-derived organoids and acetylated- $\alpha$  tubulin<sup>+</sup> (ACT<sup>+</sup>) organoids as marker for airway-derived organoids, where DAPI is blue, SPC is green, and ACT is red. Shown are organoids stimulated with 200 ng/mL HMGB1. The number per well (*C*) and the size of organoids (*D*) were measured using light microscopy. White scale bars represent 500  $\mu$ m. Data are shown as mean  $\pm$  SE, with all experiments representing 6 independent experiments. Significant difference was tested using a Mann–Whitney *U* test, \**P* < 0.05.

organoids expressing the airway marker ACT while limiting the number of organoids expressing the alveolar marker SPC.

### LL-37 Reduces the Wound Healing Capacity of A549 Cells via RAGE-Signaling

Finally, to investigate the effect of RAGE ligands on alveolar cell repair in human cells, alveolar epithelial A549 cells

were wounded using electroporation, upon which the recovery of the monolayer was monitored by measuring the trans-epithelial resistance. A549 cells were stimulated with 20  $\mu$ g/mL LL-37 1 h before electroporation. LL-37 impaired the repair response, as cells were no longer able to fully recover and form an intact monolayer. To assess whether this reduced regenerative response was caused by activation of

**Figure 5.** Receptor for advanced glycation end-products (RAGE) ligands induce alveolar tissue damage whereas RAGE inhibitors prevent elastase-induced tissue damage in murine precision cut lung slices (PCLS). *A*: graphical representation of the experimental setup. *B*: fluorescent RAGE (green) and DAPI (blue) staining in untreated PCLS and PCLS treated with 20  $\mu$ g/mL LL-37 or 200 ng/mL HMGB1 for 24 h show that RAGE expression is located and limited to alveolar epithelial cells in murine PCLS in all conditions. PCLS negative control depicts an untreated PCLS stained with DAPI. *C*: murine PCLS were treated with 1  $\mu$ g/mL of the RAGE inhibitor FPS-ZM1 for 1 h before being stimulated with or without 20  $\mu$ g/mL LL-37 or 200 ng/mL HMGB1 for 24 h. Afterward the linear mean intercept (LMI) as marker for alveolar tissue damage, was calculated in hematoxylin and eosin (H&E)-stained sections of the PCLS. *D*: PCLS were treated with 2.5  $\mu$ g/mL porcine pancreas elastase for 24 h. LMI was determined in H&E-stained sections afterward. One hour before (pretreatment) or 24 h after (post-treatment) elastase treatment, PCLS were treated with 1  $\mu$ g/mL FPS-ZM1 for 24 h. Afterward the LMI is measured in H&E-stained sections. White scale bars represent 200  $\mu$ m. Data shown as means  $\pm$  SE, all experiments are performed 6–8 times. Significance was tested using a Mann–Whitney *U* test, \**P* < 0.05 and \*\*\**P* < 0.001. [Image created with BioRender and published with permission.]

RAGE, cells were pretreated with the RAGE inhibitor FPS-ZM1 for 1 h. This significantly attenuated the LL-37-induced repair defect (Fig. 7A), indicating that this response is at least partly dependent on RAGE signaling. To confirm that the reduced repair capacity is RAGE dependent, A549 cells were transfected with RAGE-specific siRNAs. Silencing of RAGE did not alter the regenerative capacity at baseline. However, upon stimulation with LL-37, silencing of RAGE prevented the reduced repair responses (Fig. 7B), further establishing that the LL-37-induced decrease in A549 repair capacity is RAGE dependent.

## DISCUSSION

We demonstrate an additional role for the RAGE ligands LL-37 and HMGB1 in emphysema, not only inducing neutrophilic inflammation but also contributing to alveolar tissue damage and impairing alveolar epithelial repair. LL-37-induced airway inflammation was completely dependent on RAGE, as demonstrated by the lack of effect in RAGE deficient mice. Using an *in vivo* mouse model, we showed that a single intranasal treatment with HMGB1 induces airway inflammation and lung tissue damage, which was stronger in mice susceptible to develop emphysema. Furthermore, using an *ex vivo* PCLS model, we showed that RAGE inhibition enhances tissue repair upon elastase-induced tissue damage. In addition, using an organoid model, we observed that RAGE activation limits the alveolar cell regenerative capacity, promoting the formation of airway organoids. Finally, we showed in human A549 cells that LL-37 impairs the alveolar epithelial wound healing response in a RAGE-dependent fashion. Together, these data indicate that RAGE signaling plays an important role in the development of alveolar tissue damage and is a potential therapeutic target for emphysema.

Previously, we have shown that LL-37 induces neutrophilia within 6 h of intranasal administration in BALB/cByJ, which were susceptible to cigarette smoke-induced emphysema, but not in nonsusceptible DBA/2J mice (2). Similarly, we now show that LL-37 and HMGB1 induce more neutrophilic airway inflammation and HMGB1 also more tissue damage in mice strains that are more susceptible to the development of emphysema when compared with nonsusceptible strains. Differences in genetic susceptibility to alveolar tissue damage in mice was previously shown in a study by Radder et al. (33) where A/J was the most susceptible strain out of 34 strains investigated for the development of cigarette smoke-induced emphysema whereas NZW/LacJ was one of the most resistant strains. These previous findings combined with our data suggest that mice genetically susceptible for alveolar damage are also susceptible to develop HMGB1-induced alveolar damage. This supports a role not only for the release of RAGE ligands but also RAGE expression in the development of emphysema upon smoking. In addition, we observed that the mean alveolar size was larger at baseline in NZW/LacJ compared with A/J mice, which may contribute the increased susceptibility to develop alveolar tissue damage. Differences in the effects of LL-37 and HMGB1 between mouse strains may be caused by differences in receptor affinity, which is dependent on the intramolecular charge of the ligand (34). In addition, the ability of ligands to

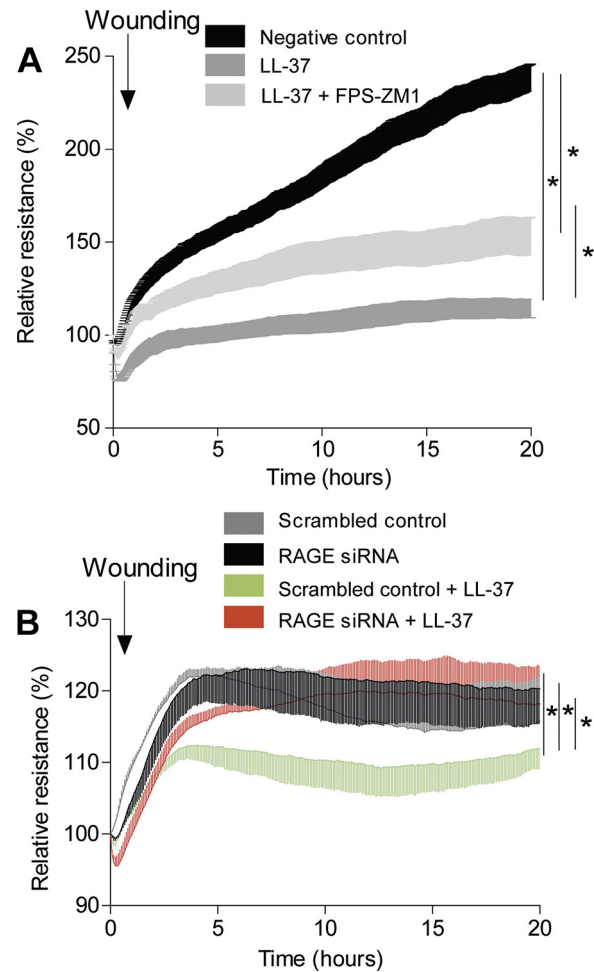


**Figure 7.** LL-37 reduces the wound healing capacity of A549 cells via receptor for advanced glycation end-products (RAGE) signaling. The alveolar epithelial adenocarcinoma cell line A549 was grown to confluency in electric cell-substrate impedance sensing (ECIS) arrays to measure the barrier function and regenerative capacity in real time. Upon reaching confluence, the cell layer was wounded using electroporation. **A:** the relative cellular resistance normalized right after the moment of electroporation to investigate the regrowth of the monolayer, or the regenerative capacity of A549 cells. Cells were stimulated with or without 20  $\mu\text{g}/\text{mL}$  LL-37 for 1 h before electroporation. In addition, cells were preincubated with 1  $\mu\text{g}/\text{mL}$  of the RAGE inhibitor FPS-ZM1 1 h before stimulation with LL-37. **B:** A549 cells were transfected with a specific siRNA assay targeting RAGE or with a scrambled siRNA assay 24 h after seeding and 48 h before wounding. A549 cells transfected with scrambled siRNA or RAGE siRNA were stimulated with 20  $\mu\text{g}/\text{mL}$  LL-37 1 h before wounding. Data are shown as mean  $\pm$  SE from 6 independent experiments. Significance was tested using a two-way ANOVA, where  $*P < 0.05$  is considered statistically significant.

activate secondary receptors, such as TLR4, and the level of expression of these receptors may also contribute to differences between strains. Previously, it was shown that C57BL/6 mice were not susceptible for the development of cigarette smoke-induced airway inflammation (6). Correspondingly, C57BL/6 mice did not show significant release of HMGB1 upon exposure to cigarette smoke for 5 days (7, 35), and we now show that HMGB1 does not induce airway inflammation in this strain, neither in wild-type C57BL/6 or RAGE and/or TLR4 gene-deficient C57BL/6 mice.

Very little is known about the effects of smoke on LL-37 release in mice, although mice lacking the murine LL-37

homologue, CRAMP (cathelicidin-related antimicrobial peptide), show significantly reduced lung immune infiltration upon exposure to cigarette smoke for 1 wk, demonstrating the importance of LL-37 in cigarette smoke-induced airway inflammation (36). Interestingly, using mice deficient in RAGE and/or TLR4, we observed a strong and completely RAGE-dependent inflammatory response upon LL-37 treatment. In addition, by using a RAGE inhibitor, we confirmed a crucial role for RAGE in the LL-37 effects on alveolar epithelial damage and repair responses. Interestingly, we observed that the intranasal treatment of mice with LL-37 induced dsDNA release in BAL fluid in both mouse strains whereas the intranasal treatment of mice with HMGB1 did not increase the BAL dsDNA levels. It was previously established that LL-37 is able to induce cell death (37), and may thus evoke the release of DAMPs, for example, dsDNA, whereas this has not been described for HMGB1, which mostly has immune modulating properties (38).

It has previously been shown that RAGE is important in the development of lung organoids and the differentiation of ATII cells into ATI cells in organoids (39, 40). Here, we showed that RAGE ligands support the development of organoids expressing airway markers at the expense of organoids expressing alveolar markers, reducing the total number of organoids, but increasing the average size of organoids, which may reflect impaired alveolar regeneration. Nuclear RAGE signaling has been shown crucial for DNA damage repair, limiting subsequent senescence and fibrosis (41). Furthermore, it was shown that increased ATII senescence leads to a reduction in SPC-expressing organoids (42). Therefore, it is tempting to speculate that activation of membrane-bound RAGE by LL-37 or HMGB1 reduces the DNA repair capacity of intracellular RAGE, inducing senescence and reducing SPC-positive organoids, ultimately resulting in a reduction in the alveolar regenerative capacity upon stimulation with RAGE ligands.

In agreement with earlier literature (43), we showed high levels of RAGE expression in the alveolar compartment in our ex vivo PCLS model. Here, we show that LL-37 directly induces tissue damage ex vivo, inducing a strong increase in alveolar enlargement that could be reversed in the presence of a small-molecule RAGE inhibitor. The exact mechanism of RAGE-induced alveolar damage requires further investigation, however it has been shown that RAGE-activation induces NADPH oxidase activation, causing the release of reactive oxygen species, which induces epithelial damage and delayed epithelial wound healing (44). Interestingly, the inhibition of RAGE after elastase-induced tissue damage reduced airspace enlargement, indicating that RAGE activation can impair epithelial repair responses. Thus, RAGE inhibition may not only reduce inflammation-induced tissue damage, but also promote alveolar tissue regeneration. As there is still no curative treatment available for COPD, there is an urgent need for the development of treatments promoting lung tissue regeneration. Future studies should identify whether RAGE inhibitors are able to promote lung tissue regeneration in patients with emphysematous COPD.

In summary, our study shows that activation of RAGE induces acute lung tissue damage and that inhibition of RAGE stimulates the epithelial repair response and may

induce lung tissue regeneration, which can potentially be used as a therapeutic target for patients with COPD.

## GRANTS

This study was funded by The Lung Foundation Netherlands (<https://www.longfonds.nl>), project 6.2.15.044JO received by S. D. Pouwels.

## DISCLOSURES

No conflicts of interest, financial or otherwise, are declared by the authors.

## AUTHOR CONTRIBUTIONS

S.D.P., R.G., M.B.S., and I.H.H. conceived and designed research; S.D.P., L.H., X.W., V.S.R.R.A., D.v.O., and L.J.B. performed experiments; S.D.P., L.H., X.W., V.S.R.R.A., D.v.O., and L.J.B. analyzed data; S.D.P., M.B.S., and I.H.H. interpreted results of experiments; S.D.P., V.S.R.R.A. and D.v.O. prepared figures; S.D.P. drafted manuscript; S.D.P., S.P., B.G.O., R.G., M.B.S., and I.H.H. edited and revised manuscript; S.D.P., L.H., X.W., V.S.R.R.A., D.v.O., L.J.B., S.P., B.G.O., R.G., M.B.S., and I.H.H. approved final version of manuscript.

## REFERENCES

1. Brajer-Luftmann B, Nowicka A, Kaczmarek M, Wyrzykiewicz M, Yasar S, Piorunek T, Sikora J, Batura-Gabryel H. Damage-associated molecular patterns and myeloid-derived suppressor cells in bronchoalveolar lavage fluid in chronic obstructive pulmonary disease patients. *J Immunol Res* 2019; 9708769, 2019. doi:10.1155/2019/9708769.
2. Pouwels SD, Hesse L, Faiz A, Lubbers J, Bodha PK, Ten Hacken NHT, van Oosterhout AJ, Nawijn MC, Heijink IH. Susceptibility for cigarette smoke-induced DAMP release and DAMP-induced inflammation in COPD. *Am J Physiol Lung Cell Mol Physiol* 311: L881–L892, 2016. doi:10.1152/ajplung.00135.2016.
3. Pouwels SD, Zijlstra GJ, van der Toorn M, Hesse L, Gras R, Ten Hacken NHT, Krysko DV, Vandenabeele P, de Vries M, van Oosterhout AJ, Heijink IH, Nawijn MC. Cigarette smoke-induced necroptosis and DAMP release trigger neutrophilic airway inflammation in mice. *Am J Physiol Lung Cell Mol Physiol* 310: L377–L386, 2016. doi:10.1152/ajplung.00174.2015.
4. Pouwels SD, Heijink IH, ten Hacken NHT, Vandenabeele P, Krysko DV, Nawijn MC, van Oosterhout AJ. DAMPs activating innate and adaptive immune responses in COPD. *Mucosal Immunol* 7: 215–226, 2014. doi:10.1038/mi.2013.77.
5. Kuipers MT, van der Poll T, Schultz MJ, Wieland CW. Bench-to-bedside review: Damage-associated molecular patterns in the onset of ventilator-induced lung injury. *Crit Care* 15: 235, 2011. doi:10.1186/cc10437.
6. Pouwels SD, Heijink IH, Brouwer U, Gras R, den Boef LE, Boezen HM, Korstanje R, van Oosterhout AJ, Nawijn MC. Genetic variation associates with susceptibility for cigarette smoke-induced neutrophilia in mice. *Am J Physiol Lung Cell Mol Physiol* 308: L693–L709, 2015. doi:10.1152/ajplung.00118.2014.
7. Pouwels SD, Faiz A, den Boef LE, Gras R, van den Berge M, Boezen HM, Korstanje R, Ten Hacken NHT, van Oosterhout AJM, Heijink IH, Nawijn MC. Genetic variance is associated with susceptibility for cigarette smoke-induced DAMP release in mice. *Am J Physiol Lung Cell Mol Physiol* 313: L559–L580, 2017. doi:10.1152/ajplung.00466.2016.
8. Huang X, Tan X, Liang Y, Hou C, Qu D, Li M, Huang Q. Differential DAMP release was observed in the sputum of COPD, asthma and asthma-COPD overlap (ACO) patients. *Sci Rep* 9: 19241, 2019. doi:10.1038/s41598-019-55502-2.
9. Pouwels SD, Nawijn MC, Bathoorn E, Riezebos-Brilman A, van Oosterhout AJM, Kerstjens HAM, Heijink IH. Increased serum levels of LL37, HMGB1 and S100A9 during exacerbation in COPD

- patients. *Eur Respir J* 45: 1482–1485, 2015. doi:10.1183/09031936.00158414.
10. **Zong H, Ward M, Stitt AW.** AGEs, RAGE, and diabetic retinopathy. *Curr Diab Rep* 11: 244–252, 2011. doi:10.1007/s11892-011-0198-7.
  11. **Ott C, Jacobs K, Haucke E, Navarrete Santos A, Grune T, Simm A.** Role of advanced glycation end products in cellular signaling. *Redox Biol* 2: 411–429, 2014. doi:10.1016/j.redox.2013.12.016.
  12. **Rouhiainen A, Kuja-Panula J, Tumova S, Rauvala H.** RAGE-mediated cell signaling. *Methods Mol Biol* 963: 239–263, 2013. doi:10.1007/978-1-62703-230-8\_15.
  13. **Oczypok EA, Perkins TN, Oury TD.** All the “RAGE” in lung disease: The receptor for advanced glycation endproducts (RAGE) is a major mediator of pulmonary inflammatory responses. *Paediatr Respir Rev* 23: 40–49, 2017. doi:10.1016/j.prrv.2017.03.012.
  14. **Haider SH, Oskuei A, Crowley G, Kwon S, Lam R, Riggs J, Mikhail M, Talusan A, Veerappan A, Kim JS, Caraher EJ, Nolan A.** Receptor for advanced glycation end-products and environmental exposure related obstructive airways disease: a systematic review. *Eur Respir Rev* 28: 180096, 2019. doi:10.1183/16000617.0096-2018.
  15. **Khaket TP, Kang SC, Mukherjee TK.** The potential of receptor for advanced glycation end products (RAGE) as a therapeutic target for lung associated diseases. *Curr Drug Targets* 20: 679–689, 2019. doi:10.2174/1389450120666181120102159.
  16. **Castaldi PJ, Cho MH, Litonjua AA, Bakke P, Gulsvik A, Lomas DA, Anderson W, Beaty TH, Hokanson JE, Crapo JD, Laird N, Silverman EK; COPD Gene and Eclipse Investigators.** The association of genome-wide significant spirometric loci with chronic obstructive pulmonary disease susceptibility. *Am J Respir Cell Mol Biol* 45: 1147–1153, 2011. doi:10.1165/rcmb.2011-0055OC.
  17. **Repapi E, Sayers I, Wain LV, Burton PR, Johnson T, Obeidat M et al.** Genome-wide association study identifies five loci associated with lung function. *Nat Genet* 42: 36–44, 2010. doi:10.1038/ng.501.
  18. **Sirisinha S.** Insight into the mechanisms regulating immune homeostasis in health and disease. *Asian Pac J Allergy Immunol* 29: 1–14, 2011.
  19. **Stogsdill MP, Stogsdill JA, Bodine BG, Fredrickson AC, Sefcik TL, Wood TT, Kasteler SD, Reynolds PR.** Conditional overexpression of receptors for advanced glycation end-products in the adult murine lung causes airspace enlargement and induces inflammation. *Am J Respir Cell Mol Biol* 49: 128–134, 2013. doi:10.1165/rcmb.2013-0013OC.
  20. **Sambamurthy N, Leme AS, Oury TD, Shapiro SD.** The receptor for advanced glycation end products (RAGE) contributes to the progression of emphysema in mice. *PLoS One* 10: e0118979, 2015. doi:10.1371/journal.pone.0118979.
  21. **Waseda K, Miyahara N, Taniguchi A, Kurimoto E, Ikeda G, Koga H, Fujii U, Yamamoto Y, Gelfand EW, Yamamoto H, Tanimoto M, Kanehiro A.** Emphysema requires the receptor for advanced glycation end-products triggering on structural cells. *Am J Respir Cell Mol Biol* 52: 482–491, 2015. doi:10.1165/rcmb.2014-0027OC.
  22. **Sanders KA, Delker DA, Huecksteadt T, Beck E, Wuren T, Chen Y, Zhang Y, Hazel MW, Hoidal JR.** RAGE is a critical mediator of pulmonary oxidative stress, alveolar macrophage activation and emphysema in response to cigarette smoke. *Sci Rep* 9: 231, 2019. doi:10.1038/s41598-018-36163-z.
  23. **Lee H, Park J-R, Kim WJ, Sundar IK, Rahman I, Park S-M, Yang SR.** Blockade of RAGE ameliorates elastase-induced emphysema development and progression via RAGE-DAMP signaling. *FASEB J* 31: 2076–2089, 2017. doi:10.1096/fj.201601155R.
  24. **Allam VSRR, Faiz A, Lam M, Rathnayake SNH, Ditz B, Pouwels SD, Brandsma CA, Timens W, Hiemstra PS, Tew GW, Neighbors M, Grimbaldston M, van den Berge M, Donnelly S, Phipps S, Bourke JE, Sukkar MB.** RAGE and TLR4 differentially regulate airway hyperresponsiveness: implications for COPD. *Allergy* 2020 76: 1123–1135, 2021. doi:10.1111/all.14563.
  25. **Ng-Blichfeldt J-P, Schrik A, Kortekaas RK, Noordhoek JA, Heijink IH, Hiemstra PS, Stolk J, Königshoff M, Gosens R.** Retinoic acid signaling balances adult distal lung epithelial progenitor cell growth and differentiation. *EBioMedicine* 36: 461–474, 2018. doi:10.1016/j.ebiom.2018.09.002.
  26. **Wu X, van Dijk EM, Ng-Blichfeldt J-P, Bos IST, Ciminieri C, Königshoff M, Kistemaker LEM, Gosens R.** Mesenchymal WNT-5A/5B signaling represses lung alveolar epithelial progenitors. *Cells* 8: 1147, 2019. doi:10.3390/cells8101147.
  27. **Thurlbeck WM.** Measurement of pulmonary emphysema. *Am Rev Respir Dis* 95: 752–764, 1967. doi:10.1164/arrd.1967.95.5.752.
  28. **van der Strate BWA, Postma DS, Brandsma C-A, Melgert BN, Luinge MA, Geerlings M, Hylkema MN, van den Berg A, Timens W, Kerstjens HA.** Cigarette smoke-induced emphysema: a role for the B cell? *Am J Respir Crit Care Med* 173: 751–758, 2006. doi:10.1164/rccm.200504-594OC.
  29. **Hou S, Tian T, Qi D, Sun K, Yuan Q, Wang Z, Qin Z, Wu Z, Chen Z, Zhang J.** S100A4 promotes lung tumor development through  $\beta$ -catenin pathway-mediated autophagy inhibition. *Cell Death Dis* 9: 277, 2018. doi:10.1038/s41419-018-0319-1.
  30. **Peng Y, Horwitz N, Lakatta EG, Lin L.** Mouse RAGE variant 4 is a dominant membrane receptor that does not shed to generate soluble RAGE. *PLoS One* 11: e0153657, 2016. doi:10.1371/journal.pone.0153657.
  31. **Takino J-I, Yamagishi S-I, Takeuchi M.** Cancer malignancy is enhanced by glyceraldehyde-derived advanced glycation end-products. *J Oncol* 2010: 739852, 2010. doi:10.1155/2010/739852.
  32. **Faiz A, Heijink IH, Vermeulen CJ, Guryev V, van den Berge M, Nawijn MC, Pouwels SD.** Cigarette smoke exposure decreases CFLAR expression in the bronchial epithelium, augmenting susceptibility for lung epithelial cell death and DAMP release. *Sci Rep* 8: 12426, 2018. doi:10.1038/s41598-018-30602-7.
  33. **Radder JE, Gregory AD, Leme AS, Cho MH, Chu Y, Kelly NJ, Bakke P, Gulsvik A, Litonjua AA, Sparrow D, Beaty TH, Crapo JD, Silverman EK, Zhang Y, Berndt A, Shapiro SD.** Variable susceptibility to cigarette smoke-induced emphysema in 34 inbred strains of mice implicates Abi3bp in emphysema susceptibility. *Am J Respir Cell Mol Biol* 57: 367–375, 2017. doi:10.1165/rcmb.2016-0220OC.
  34. **Fritz G.** RAGE: a single receptor fits multiple ligands. *Trends Biochem Sci* 36: 625–632, 2011. doi:10.1016/j.tibs.2011.08.008.
  35. **Pouwels SD, Heijink IH, van Oosterhout AJM, Nawijn MC.** A specific DAMP profile identifies susceptibility to smoke-induced airway inflammation. *Eur Respir J* 43: 1183–1186, 2014. doi:10.1183/09031936.00127813.
  36. **Li D, Beisswenger C, Herr C, Schmid RM, Gallo RL, Han G, Zakharkina T, Bals R.** Expression of the antimicrobial peptide cathelicidin in myeloid cells is required for lung tumor growth. *Oncogene* 33: 2709–2716, 2014. doi:10.1038/ncr.2013.248.
  37. **Bankell E, Dahl S, Gidlöf O, Svensson D, Nilsson B-O.** LL-37-induced caspase-independent apoptosis is associated with plasma membrane permeabilization in human osteoblast-like cells. *Peptides* 135: 170432, 2021. doi:10.1016/j.peptides.2020.170432.
  38. **Kianian F, Kadkhodae M, Sadeghipour HR, Karimian SM, Seifi B.** An overview of high-mobility group box 1, a potent pro-inflammatory cytokine in asthma. *J Basic Clin Physiol Pharmacol* 31: 20190363, 2020. doi:10.1515/jbcpp-2019-0363.
  39. **Katsura H, Kobayashi Y, Tata PR, Hogan BLM.** IL-1 and TNF $\alpha$  contribute to the inflammatory niche to enhance alveolar regeneration. *Stem Cell Rep* 12: 657–666, 2019. doi:10.1016/j.stemcr.2019.02.013.
  40. **Sun T, Huang Z, Zhang H, Posner C, Jia G, Ramalingam TR, Xu M, Brightbill H, Egen JG, Dey A, Arron JR.** TAZ is required for lung alveolar epithelial cell differentiation after injury. *JCI Insight* 5, 2019. doi:10.1172/jci.insight.128674.
  41. **Kumar V, Fleming T, Terjung S, Gorzelanny C, Gebhardt C, Agrawal R, Mall MA, Ranzinger J, Zeier M, Madhusudhan T, Ranjan S, Isermann B, Liesz A, Deshpande D, Häring HU, Biswas SK, Reynolds PR, Hammes HP, Peperkok R, Angel P, Herzog S, Nawroth PP.** Homeostatic nuclear RAGE-ATM interaction is essential for efficient DNA repair. *Nucleic Acids Res* 45: 10595–10613, 2017. doi:10.1093/nar/gkx705.
  42. **Lehmann M, Hu Q, Hu Y, Hafner K, Costa R, van den Berg A, Königshoff M.** Chronic WNT/ $\beta$ -catenin signaling induces cellular senescence in lung epithelial cells. *Cell Signal* 70: 109588, 2020. doi:10.1016/j.cellsig.2020.109588.
  43. **Kasper M, Seidel D, Knels L, Morishima N, Neisser A, Bramke S, Koslowski R.** Early signs of lung fibrosis after in vitro treatment of rat lung slices with CdCl<sub>2</sub> and TGF- $\beta$ 1. *Histochem Cell Biol* 121: 131–140, 2004. doi:10.1007/s00418-003-0612-6.
  44. **Shi L, Chen H, Yu X, Wu X.** Advanced glycation end products delay corneal epithelial wound healing through reactive oxygen species generation. *Mol Cell Biochem* 383: 253–259, 2013. doi:10.1007/s11010-013-1773-9.